JOURNAL OF APPLIED POLYMER SCIENCE VOL. 15, PP. 2471–2485 (1971)

Unidirectional Fiber–Polymer Composites: Swelling and Modulus Anisotropy

A. Y. CORAN, K. BOUSTANY, and P. HAMED,
Monsanto Company, Rubber Chemicals Research Laboratories, Akron, Ohio 44313

Synopsis

The solvent swelling of unidirectional rubber–fiber composites was studied. The amount of matrix swelling was constrained to the extent that would be predicted from the thermodynamic theories of elasticity and polymer–solvent interaction. The geometry of swelling was found to be orthotropic in nature. A simple trigonometric function was derived to relate linear deformation due to swelling to the angle which the direction of its measurement makes with the fiber direction. The validity of the derivation was demonstrated experimentally. Considering swelling to be the imposition of tensile forces of equal magnitude in all directions, and considering a swelling-induced linear deformation to be analogous to a tensile compliance, a simple set of relationships between elastic parameters and their direction of measurement was derived:

$$\frac{1}{E_\theta} = \frac{\cos^2\theta}{E_L} + \frac{\sin^2\theta}{E_T}$$

$$G_\theta = G_{LT}$$

$$\nu_\theta = \nu_{LT}\frac{E_\theta}{E_L}$$

$$\eta_\theta = E\left(\frac{1}{E_T} - \frac{1}{E_L}\right)\cos\theta\sin\theta$$

where E_θ, G_θ, ν_θ, and η_θ are Young's modulus, shear modulus, Poisson's ratio, and the shear coupling ratio measured in a longitudinal transverse plane at an angle with the fiber direction, respectively, and E_L, G_{LT}, and θ_{LT} are the longitudinal Young's modulus, the longitudinal transverse shear modulus, and the longitudinal transverse Poisson ratio, respectively. Further simplifying the case of combined transverse isotropy and special orthotropy was the conclusion that $1/G_{LT} = 1/E_T + (1 + 2\nu_{LT})/E_L$. The relationships for G and E were experimentally demonstrated.

INTRODUCTION

Composites consisting of high-modulus fibers imbedded unidirectionally in softer matrixes are anisotropic in such properties as strength, ultimate elongation, and Young's modulus.[1] In addition, if the matrix is a cross-linked polymer which can be swollen by a solvent, the swelling of the composite will be anisotropic; it will swell to the greatest extent in directions perpendicular or transverse to the fiber direction.

The work reported here started as a study of the swelling of unidirectional fiber–rubber composites. Swelling was considered to be constrained in one direction only. The amount of swelling at equilibrium was treated as a special case of the Flory-Rehner theory.[2]

The geometry of swelling was also considered. From studies of swelling geometry, the relationship between linear deformation due to swelling and its direction of measurement became apparent. Swelling was considered as a model for the application of stresses of equal magnitude in all directions. From this model, equations for the moduli of unidirectional composites were derived.

THEORY

The Amount of Solvent Imbibed

According to the Flory-Rehner theory for the swelling of a rubbery polymer, at equilibrium,

$$\ln(1 - v_r) + v_r + \chi v_r^2 + \nu_e V_1 (v_r^{1/3} - v_r/2)/V_0, = 0 \qquad (1a)$$

where v_r is the volume fraction of rubber after swelling, χ is the polymer–solvent interaction parameter, ν_e is the number of "moles" of effective network chains in the initial or unswollen volume V_0, and V_1 is the molar volume of solvent. The relationship of eq. (1a) is for the swelling of unconstrained rubber; however, if the rubber is constrained in two directions and can only swell in one direction, eq. (1a) becomes

$$\ln(1 - v_r) + v_r + \chi v_r^2 + \nu_e V_1 (1/v_r - v_r/2)/V_0 = 0. \qquad (1b)$$

Similarly, if constraint is in one direction and swelling can occur in the other two directions, we obtain

$$\ln(1 - v_r) + v_r + \chi v_r^2 + \nu_e V_1 (1 - v_r/2)/V_0 = 0. \qquad (1c)$$

Equations (1a), (1b), and (1c) are not unlike those given by Treloar.[3] They differ only in the presence of the second term of the bracketed coefficient of ν_e, $-v_r/2$.

In this work, use will be made of eq. (1c). Unidirectional constraint will be accomplished by the incorporation of a relatively low concentration of unidirectionally oriented fibers.

Swelling Geometry

In the above, it was assumed that swelling would not occur along the lengths of the fibers. This, of course, would be applicable only to very long fibers of infinitely high Young's modulus. It was also assumed that the distance between the fibers would increase uniformly. This would imply that if a specimen were prepared such that all of the surfaces of the specimen were either parallel or perpendicular to the fiber axes, as in Figure 1 (specially orthotropic), after swelling the surfaces would still be parallel or per-

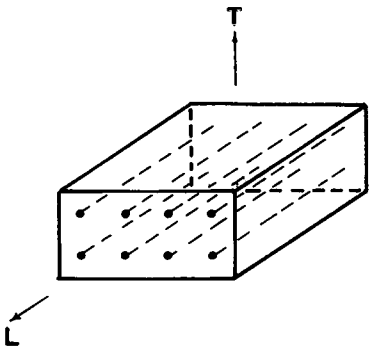

Fig. 1. Schematic diagram of a transversely isotropic specially orthotropic composite structure.

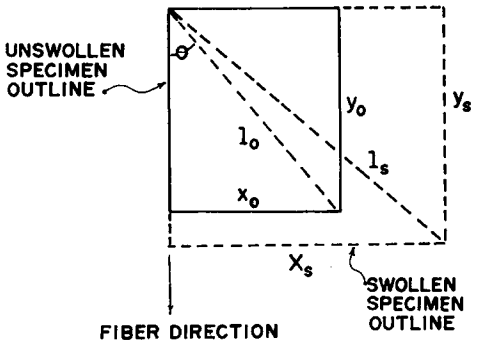

Fig. 2. Geometry of the swelling of unidirectional composites.

pendicular. In a practical case, at least a small amount of lengthening of the fibers would have to occur since no fiber has infinite modulus.

Figure 2 is a representation of a unidirectional composite specimen before (solid lines) and after (dotted lines) swelling. The length of the line of length l_0 taken at an angle θ with the fiber direction grows during swelling to a length l_s. If $x_s/x_0 = a_T$, $y_s/y_0 = a_L$, and $l_s/l_0 = a_\theta$, then

$$a_\theta = [(a_T^2 - a_L^2) \sin^2\theta + a_L^2]^{1/2}. \tag{2}$$

The Distribution of Young's Modulus with Angle θ

Consider now that swelling is a uniform stress applied against an elastic network which is partially constrained by fibers bonded to the network or matrix. If the amount of swelling is small,

$$E_\theta = \frac{K}{a_\theta - 1}, \tag{3}$$

where E_θ is Young's modulus of the composite measured at an angle θ with the fibers and K is a proportionality constant (in units of force per area). Of course, we should think in terms of rather poor solvents so that the small

deformations will indeed be proportional to the applied force represented by K.

Substituting eq. (2) into eq. (3), we obtain

$$\frac{1}{E_\theta} = \{[(a_T^2 - a_L^2)\sin^2\theta + a_L^2]^{1/2} - 1\}/K. \tag{4}$$

For small amounts of swelling we can write

$$a_T = 1 + \frac{K}{E_T} \tag{5}$$

and

$$a_L = 1 + \frac{K}{E_L} \tag{6}$$

Then, since strains are small,

$$a_T^2 \approx 1 + \frac{2K}{E_T} \tag{7}$$

and

$$a_L^2 \approx 1 + \frac{2K}{E_L}. \tag{8}$$

Equation (4) now becomes

$$\frac{1}{E_\theta} = \left\{\left[2K\left(\frac{1}{E_T} - \frac{1}{E_L}\right)\sin^2\theta + 1 + \frac{2K}{E_L}\right]^{1/2} - 1\right\}\Big/K. \tag{9}$$

The consideration of only small strains enables further the approximation

$$\left[1 + 2K\left(\frac{1}{E_T} - \frac{1}{E_L}\right)\sin^2\theta + \frac{2K}{E_L}\right]^{1/2} \approx 1 + \left(\frac{1}{E_T} - \frac{1}{E_L}\right)\sin^2\theta + \frac{K}{E_L}. \tag{10}$$

Thus, eq. (9) becomes

$$\frac{1}{E_\theta} = \left(\frac{1}{E_T} - \frac{1}{E_L}\right)\sin^2\theta + \frac{1}{E_L}$$

or, alternately,

$$\frac{1}{E_\theta} = \frac{\cos^2\theta}{E_L} + \frac{\sin^2\theta}{E_T}. \tag{11a}$$

This is the same as the relationship given by Horio and Onogi which related the modulus of paper to fiber orientation.[4]

Equation (10) is less complex than the frequently used equation

$$\frac{1}{E_\theta} = \frac{\cos^4\theta}{E_L} + \left(\frac{1}{G_{LT}} - \frac{2\,\nu_{LT}}{E_L}\right)\sin^2\theta\cos^2\theta + \frac{\sin^4\theta}{E_T}, \tag{12}$$

where G_{LT} is the longitudinal transverse shear modulus and ν_{LT} is the corresponding Poisson ratio.[5,6] Equation (12) was derived from a fourth-order tensor transformation of the compliances in orthotropic materials, while eq. (10) was derived from a description of the distribution of strains in a unidirectional or transversely isotropic specially orthotropic composite which results from the application of a uniform hydrostatic strain. The requirement of combined transverse isotropy and special orthotropy associated with eq. (11a) would tend to simplify the relationships between compliance or stiffness and orientation. Indeed it can be readily shown that eq. (11a) is identical to eq. (12) if the following condition is met:

$$\frac{1}{G_{LT}} = \frac{1}{E_T} + \frac{(1 + 2\nu_{LT})}{E_L}. \tag{13}$$

If $E_T = E_L$, eq. (13) becomes the classical relationship $1/G = 2(1 + \nu)/E$. Further, if the condition expressed in eq. (13) is imposed on the other equations which are associated with eq. (12), the following relationships for transversely isotropic specially orthotropic composites are obtained:

$$G_\theta = G_{LT} \tag{11b}$$

$$\nu_\theta = \nu_{LT} \frac{E_\theta}{E_L} \tag{11c}$$

$$\eta_\theta = E_\theta \left(\frac{1}{E_T} - \frac{1}{E_L} \right) \cos\theta \sin\theta \tag{11d}$$

where η_θ is the shear coupling coefficient measured at angle θ.

Equations (11a), (11b), (11c), and (11d) no doubt relate only to transversely isotropic specially orthotropic composites; however, it should be noted that the unidirectional composite is very commonly used.

EXPERIMENTAL RESULTS AND DISCUSSION

Swelling Constraint in Unidirectional Rubber–Tire Cord Composites

The swelling of vulcanized gum rubber in toluene was constrained unidirectionally by the embedment of rayon tire cords. Compositions for the swelling measurements were prepared according to the recipes in Table I. Compositions I, II, and III were matrix compositions of low, medium, and high crosslink densities, respectively. The corresponding unidirectional composites were designated I-C, II-C, and III-C. The matrix compositions were mixed on a differential roll mill and sheeted off about 0.025 in. thick. The unfilled matrix stocks were molded in a cavity mold and cured in the form of strips 0.1 in. thick and 0.38 in. wide. Strips were cut into lengths of about 2 in.

The composites were prepared by imbedding rayon tire cord fabric between the 0.025-in.-thick milled sheets of matrix compositions to form sandwich plies. The plies were stacked unidirectionally in the cavity mold and cured. The rayon tire cord fabric was coated with resorcinol–formalde-

TABLE I
Constrained Swelling in Unidirectional Rubber–Tire Cord Composites[a]

	I	II	III	I-C	II-C	III-C
Matrix parts, by wt						
Natural rubber	100.	100.	100.	100.	100.	100.
Zinc oxide	5.	5.	5.	5.	5.	5.
Stearic acid	3.	3.	3.	3.	3.	3.
Sulfur	1.	2.	4.	1.	2.	4.
N-*t*-Butylbenzothiazolesulfenamide	0.25	0.5	1.0	0.25	0.50	1.0
Fibers, vol-%						
Rayon tire cord, RFL Coated (0.0069 g/in.)	0.0	0.0	0.0	20.2	21.5	19.9
Apparent density of cord in rubber	—	—	—	1.32	1.23	1.24
Swelling data						
a_x (transverse)	1.94	1.71	1.59	2.10	1.84	1.69
a_z (transverse)	1.97	1.72	1.61	2.15	1.84	1.73
a_y (longitudinal)	2.05	1.74	1.60	1.00	1.00	1.00
v_r from linear measurements	0.124	0.187	0.233	0.178	0.238	0.282
v_r from weight measurements	0.128	0.185	0.234	0.159	0.225	0.274

[a] See text for composite designations.

hyde–latex (RFL) to promote adhesion. Curing of matrix and composite compositions was at 153°C for 25 min.

Weights of the compositions before and after swelling in toluene were determined on an analytical balance. Measurements of swollen and unswollen widths and thicknesses were made by a gauge micrometer. Lengths were measured by a ruler. There is some uncertainty in the length measurements due to the fact that some bulging occurred between the cords. However, it was judged that this amounted to less than 1% of the length. No lengthening of the cords themselves was measurable.

The volume per cent of rayon cord was estimated on the basis of the total length imbedded in a specimen. This enabled the estimation of the weight of cord. The coated cord weighed 0.0069 g/in. Since both linear and weight measurements of composite specimens were made, densities of the matrices and composites were apparent and the volume per cent of cord was calculated. The density of the imbedded cord was found to be somewhat less than was expected (1.23 to 1.32 instead of 1.52). This was, no doubt, due to a small amount of air trapped between the cord fibers under the RFL coating.

The volume fraction of rubber, v_r, was calculated from the linear deformations (a_x, a_y, and a_z) as well as from weight measurements. The calculations were as follows:

$$v_r \text{ (from linear deformations)} = \frac{1 - v_{nn}}{a_x a_y a_z - v_{nn}} \tag{14}$$

and

$$v_r \text{ (from weight measurements)} = (1 - v_{nn}) \Big/ \left[\left(\frac{M_s}{M_0} - 1 \right) \frac{\rho_{\text{solv}}}{\rho_{\text{comp}}} + 1 - v_{nn} \right] \quad (15)$$

where v_{nn} is the volume fraction of nonnetwork matter (zinc oxide, stearic acid, cords, etc.), M_s is the swollen weight of the composite, M_0 is the unswollen weight, ρ_{solv} is the density of solvent, and ρ_{comp} is the density of the composite.

Before swelling, the surfaces of the specimen strips were either parallel or perpendicular to the direction of the cords. This was also true after swelling, although some surface ripples similar to those noted by Southern and Thomas[8] (in biaxially constrained swelling) did occur. The ripples were in the form of small inward folds which ran in the transverse direction.

The results of this portion of the work are given in Table I. The constraint due to the presence of the tire cords was considered purely unidirectional in the present treatment. The two-dimensional constraint which undoubtedly occurs in regions of the rubber matrix adjacent to the cords was ignored; however, its effect would be small with the relatively low concentrations of cord used. It is interesting to note that, although the constraint reduces the amount of solvent imbibed, the linear deformations in the "unconstrained" direction actually increase.

The values of v_r in the constrained composites (I-C, II-C, and III-C) were plotted against the values of v_r obtained in the unconstrained matrix compositions (I, II, and III) in Figure 3. The solid line curve is calculated from the comparison of eqs. (1a) and (1c), using χ values from Kraus.[7] (For natural rubber swollen by toluene, $\chi = 0.43 + 0.05v_r$.) The experimental points are quite close to the theoretical curves, thus indicating good agreement between experiment and theory. The dotted line curve in Figure 3 is the relationship between uniaxially constrained and unconstrained swelling which one obtains using Treloar's formulation. The two curves are so close together that it is impossible to decide which formulation is more nearly correct. At any rate, the present results are in agreement with both the Treloar and the Flory-Rehner approach.

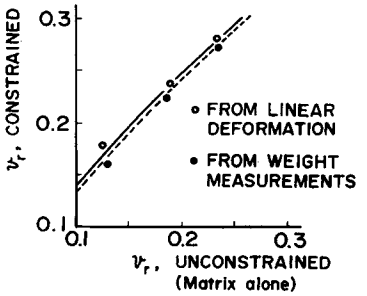

Fig. 3. Relationship between unidirectionally cnostrained and unconstrained swelling.

Swelling Geometry

Strips of unidirectional rubber–fiber composite were cut at various angles (θ) with the fiber direction and swollen in toluene. The change in swollen length with θ was studied. However, the tire cord composites were not considered well suited for this work for two reasons. In the case of the tire cord composite, there was practically no swelling in the direction of the cords; hence, the amounts of linear deformation associated with small values of θ would be difficult to measure. Also the distance between cords is large enough to give irregularities in the swollen direction.

For these reasons, a composite composition containing discontinuous glass fiber was used. The recipe is as follows:

	Parts by wt
SBR 1502	100
Carbon black N-285	50
Silica (HiSil 233)	15
Zinc oxide	3.0
Stearic acid	2.0
Sulfur	2.0
N-*t*-Butylbenzothiazolesulfenamide	1.0
Hexamethylenetetramine	1.6
Resorcinol	2.5
Antidegrandant	2.0
Fiberglass (8 μ diam.)	75

The rubber was mixed with the glass fibers (initially $^1/_4$ in. long) in a Brabender for 2 min using a circulating oil temperature of 50°C. The Brabender was run at 60 rpm. All of the rest of the ingredients were then added, and mixing continued another 2 min. The mass was sheeted on a differential roll mill to a thickness of about 0.15 in. The mill was then set to give a 0.075-in.-thick sheet. The 0.15-in.-thick sheet was then passed once, then doubled and passed again. The sheet was then doubled and passed seven additional times keeping the direction of work constant. Thus, an oriented sheet was produced.

The oriented sheet was cured between platens at 153°C for 35 min under a pressure of about 200 psi. Aluminum foil was used between the composite and platens to facilitate extraction from the press. The outer edges of the composite were trimmed away since the curing pressure was too low near the edges (about $^1/_2$ in. was trimmed).

After curing, the sheet was nicked and torn in a longitudinal direction. The tear followed the direction of orientation. This established the average fiber direction. Microscopic observation along the tear revealed that the orientation was good (fiber directions deviated from one another by no more than 10 degrees) and that the fiber lengths were reduced to about 200 μ.

Strips were die cut at various angles with the fiber direction established by the tear. The strips were 2.00 in. long, about 0.075 in. wide, and 0.070

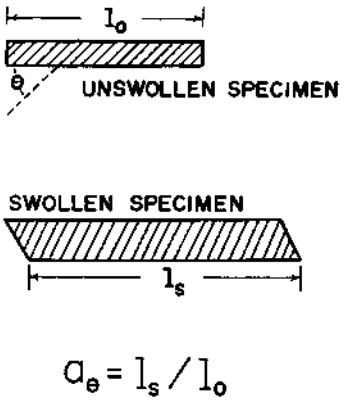

Fig. 4. Measurement of swelling-induced linear deformations.

in. thick. The specimen strips were swollen in toluene for one day. Lengths were measured before and after swelling. Thus, a_θ was determined. It should be noted that, although the strips were all rectangular before swelling, strips cut at angles between 0 and 90 degrees were no longer rectangular after swelling, although opposing surfaces remained planar and parallel. This is illustrated by Figure 4. In addition to the above measurements, a_z in the direction normal to the curing platens was determined. If the composite were truly unidirectional, a_z would equal a_x.

Before considering the results, a little might be said about the composite recipe. The silica, hexamethylenetetramine, and resorcinol were incorporated to promote the adhesion of fibers to the matrix.[9] The crosslink density, which is determined by the concentrations of sulfur and accelerator (N-*t*-butylbenzothiazolesulfenamide), was adjusted to give composites which would swell to give conveniently measurable deformations. The data are given in Table II.

TABLE II
Linear Swelling Deformations for Various Fiber Orientations

Orientation θ, degrees	a_θ	a_z
0	1.041(a_y)	1.56
15	1.063	1.57
30	1.128	1.56
45	1.243	1.58
60	1.347	1.56
75	1.433	1.56
90	1.468(a_x)	1.54

The values obtained for a_z are all very close. This indicates good uniformity in the composite preparation. It is interesting that a_z (average value 1.558) is not the same as a_x. Swelling in the direction normal to the curing platens is greater than in the other transverse direction. This is

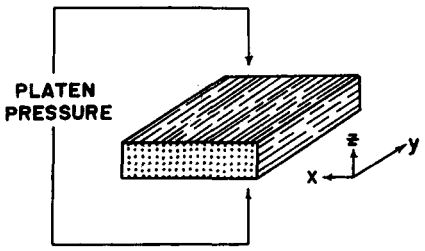

Fig. 5. Application of force during curing.

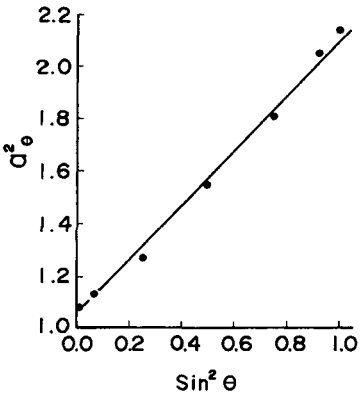

Fig. 6. Relationship between swelling-induced linear deformation and fiber orientation.

probably due to the slight flow which occurred during pressing. This would tend to slightly disrupt the fibers in the xy plane but slightly purify the orientation in the zy plane (Fig. 5). It is thus evident that the composites prepared in the above manner are not completely unidirectional, although they are nearly so.

The surface characteristics of the swollen discontinuous composites differed from those of the continuous tire cord composites. There was none of the rippling which occurred in the tire cord composites. Just a slight grain pattern appeared in the direction of the fibers.

Specimens wherein θ was 0 or 90 degrees remained rectangular. Therefore, the relationship of eq. (2) should hold. A plot of a_θ^2 against $\sin^2\theta$ should be a straight line of slope, $a_T^2 - a_L^2$, and intercept a_L^2. Figure 6 is such a plot from the data in Table II. The slope is 1.02 and the intercept is 1.08. Values of a_θ calculated from eq. (2) and the slope and intercept values from Figure 6 differ from experimental values by only 0.013 on the average. Equation (2) is, then, a reasonable description of swelling anisotropy.

The Distribution of Modulus with Angle θ

Specimens for the study of the distribution of Young's modulus with θ were prepared from the same short fiber composite as that used in the study

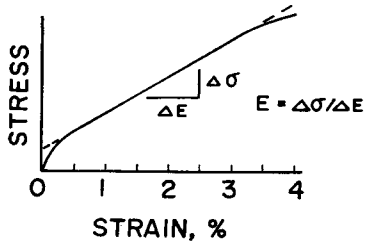

Fig. 7. Typical stress–strain curve for the glass fiber–rubber composites.

of the distribution of swelling deformations. Short fibers were chosen because it was felt that in cutting the tensile strips at various angles with the fiber axis, continuous or long fibers would be greatly shortened. For example, the tire cord composite would give specimens with effective fiber aspect ratios ranging from infinity (for $\theta = 0$) to about 20 (for $\theta = 90$ degrees). Since rubber has a low modulus, the effect on E would be extreme.

"Dog bone" shaped specimens were die cut from the short (aspect ratio = about 20) fiber glass composite. The test sections measured 2.00 in. × 0.07 in. × 0.07 in. An Instron tester was used. The cross head travelled at a rate of 0.20 in./min. Stress–strain curves of the type typified by Figure 7 were thus generated.

The very low strain portions (less than 1%) of the curves were ignored. This initial steep portion is due to the carbon black structure in the matrix[10,11] and varies as a result of repeated nondestructive tensile strains (of about 3–5%). The slope between 1% and 3–5% strain does not change as a result of mechanical working. For these reasons, Young's modulus was taken as the slope of the straight-line portion of the curve which occurred between 1% and 5%. The test results are given in Table III.

TABLE III
The Distribution of Young's Modulus with θ

Test angle θ, degrees	Experimental E_θ, ksi	Calculated E_θ, ksi
0	16.1	16.1
15	12.1	11.7
30	6.7	6.8
45	4.0	4.3
60	2.9	3.1
75	2.7	2.6
90	2.4	2.5

Values of $1/E_\theta$ were plotted against $\sin^2\theta$. From the slope $(1/E_T - 1/E_L)$ and intercept $(1/E_L)$ of the straight line drawn through the points, average values for E_L and E_T were obtained. These were used in eq. (11a) to calculate E_θ. The calculated values are also given in Table III, where the modulus values of E_θ are in thousands of pounds per square inch (ksi).

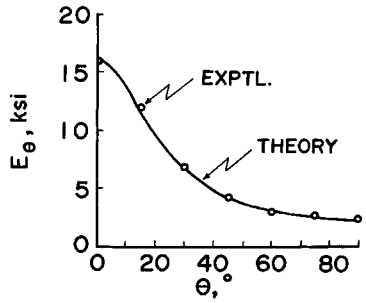

Fig. 8. E_θ as a function of θ for the glass fiber–rubber composite. Modulus values are in thousands of pounds per square inch (ksi).

Experimental values of E_θ are also compared to theory in Figure 8. The agreement between the experimental results and theory is good.

The plots of Figures 9 and 10 compare experimental values of E_θ with calculated values for continuous glass fiber–epoxy and carbon fiber–epoxy unidirectional composites. The experimental results were from Lavengood[12] and Dimmock and Abrahams.[13] As before, the values for E_L and E_T used in the calculation were obtained by finding the slope and intercept from plots of $1/E_\theta$ versus $\sin^2\theta$. In both cases the agreement with theory is good. This indicates that eq. (11a) can be applied to composites having hard matrices; also, it can be applied to continuous fiber composites.

The present theory predicts an invariant longitudinal transverse shear modulus, G_θ. To test this, specimens of the short glass fiber–rubber composite were sheared by the Instron tester. The position of the specimen in the tester jaws is given by Figure 11. The 0.07-in.-thick circular specimen was 1.50 in. in diameter, but in the calculation of G, a length of 1.4 was used for the area of shear. The specimen was clamped in flat, roughened jaws.

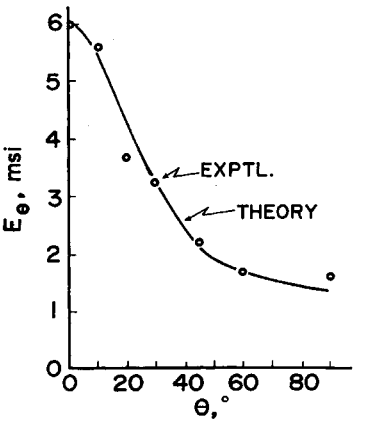

Fig. 9. E_θ as a function of θ for a glass fiber–epoxy composite. Modulus values are in millions of pounds per square inch (msi).

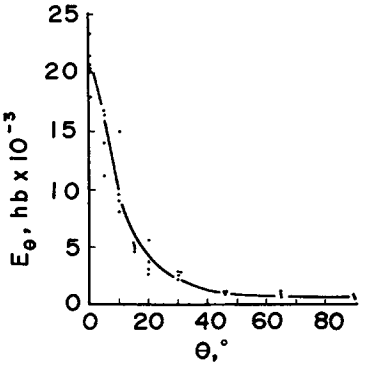

Fig. 10. E_θ as a function of θ for a carbon fiber-epoxy composite. Modulus values are in hectobars (1 hb = 1.45 ksi).

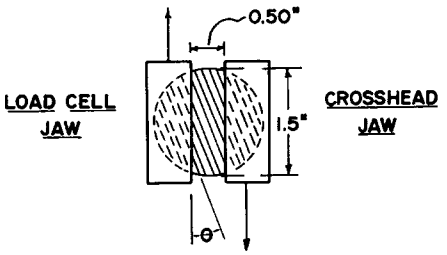

Fig. 11. Shear specimen in tensile tester jaws.

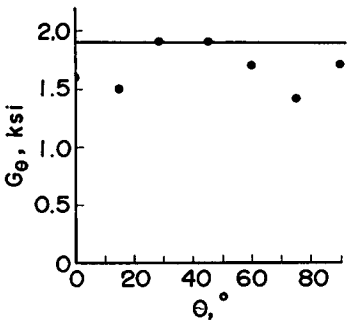

Fig. 12. Shear modulus as a function of fiber orientation.

The lower jaw was rigidly attached to the cross head, whereas the upper or load cell jaw hung from a universal joint. The cross head traveled at a rate of 0.02 in./min. The slope of the straight-line portion of the stress–strain curve which occurs near the origin was used in the calculation of G. This generally occurred at strains between about 0.2% and 2%. At these low strains the clamping arrangement appeared adequate. The results are given in Figure 12. Indeed, the shear modulus appears to be invariant with θ.

A value for G_{LT} was calculated from eq. (13). For this calculation, ν_{LT} was estimated by the volume fraction rule, using a value of 0.50 for ν of the rubber matrix and a value of 0.20 for the fibers. The estimated value was 0.45. The value of G_{LT} thus calculated was 1.9 ksi. This compares well with the experimentally determined value of G_θ in Figure 12.

CONCLUSIONS

From the studies of the imbibition of a solvent into the matrix of a unidirectional fiber composite, it was concluded that the fibers restrict the amount of swelling. The amount of constraint is in agreement with what would be predicted from the thermodynamic treatment of elasticity and polymer solvent interaction.

In unidirectional composites, the swelling is orthotropic. The linear deformation due to swelling is a simple trigonometric function of the angle θ made by the direction of the measured deformation and the fiber direction.

Swelling is analogous to the imposition of tensile forces of equal magnitude in all directions simultaneously. The geometry of swelling is then analogous to the geometry of compliance or the inverse geometry of the distribution of stiffness with θ.

The relationship for Young's modulus derived from the swelling analogy is

$$\frac{1}{E} = \frac{\cos^2\theta}{E_L} + \frac{\sin^2\theta}{E_T}$$

for unidirectional or transversely isotropic specially orthotropic composites. The angle θ is always measured in reference to the fiber direction. When this relationship is equated to the relationship for the general case of orthotropic materials, the following condition for combined transverse isotropy and special orthotropy emerges:

$$\frac{1}{G_{LT}} = \frac{1}{E_T} + \frac{1 + 2\nu_{LT}}{E_L}.$$

It then follows that the shear modulus in the longitudinal transverse plane is invariant with θ and the longitudinal transverse Poisson ratio varies directly with E_θ:

$$\nu_\theta = \nu_{LT}\frac{E_\theta}{E_L}.$$

It also follows that the shear coupling ratio η_θ is a simplified function of θ:

$$\eta_\theta = E_\theta\left(\frac{1}{E_T} - \frac{1}{E_L}\right)\cos\theta\sin\theta.$$

Thus, the relationships between the elastic parameters and the direction of their measurement are, by far, less complex than for the general case of orthotropic composites.

Although rubber was used as the model matrix in this work, the relationships should apply to hard matrix composites as well.

References

1. L. J. Broutman and R. H. Krock, *Modern Composite Materials*, Addison-Wesley, Reading, Mass., 1967.

2. P. J. Flory, *Principles of Polymer Chemistry*, Cornell University Press, Ithaca, N. Y., 1953, Chaps. 11–13.

3. L. R. G. Treloar, *The Physics of Rubber Elasticity*, 2nd Ed., Oxford Univ. Press, London, 1958, Chap. 7.

4. M. Horio and S. Onogi, *J. Appl. Phys.*, **22**, 971 (1951).

5. J. M. Whitney, *Text. Res. J.*, **37**, 1056 (1967).

6. S. G. Lekhnitskii, *Theory of Elasticity of an Anisotropic Elastic Body*, Holden Day, San Francisco, 1963, pp. 1–51.

7. G. Kraus, *Rubber World*, **135**, 67 (1956).

8. E. Southern and A. G. Thomas, *J. Polym. Sci. A*, **3**, 641 (1965).

9. J. R. Creasey, D. B. Russell, and M. P. Wagner, *Rubber Chem. Technol.*, **41**, 1300 (1968).

10. W. L. Holt, *ibid.*, **5**, 79 (1932).

11. F. Bueche, *ibid.*, **34**, 493 (1961).

12. R. E. Lavengood, private communication.

13. J. Dimmock and M. Abrahams, *Composites*, **1**, 87 (1969).

Received May 12, 1971
Revised May 27, 1971